

# Enhancement of Heat Transfer Capacity of Heat Pipe Heat Sink



V. Saravanan, K. Rakshith, Vishakh, Nithesh Bhaskar, and Nataraj Badiger

## 1 Introduction

In recent years, developments in electronics field have led to high-speed electronic equipment. The effects of these developments may be commonly seen in computers. The heat dissipation from functional elements can no longer be efficiently done with the conventional approaches like passive heat sinks. Heat pipes are two-phase flow heat transfer devices where processes of liquid to vapour and vice versa circulate between evaporator to condenser with high effective thermal conductivity. Heat pipe technology has found increasing applications in enhancing the thermal performance of heat exchangers in microelectronics, energy savings in heating, ventilating, and air conditioning (HVAC) systems.

Solomon et al. [1] developed analytical expression to predict the thermal conductivity of a heat pipe based on the heat transport limit equations. The thermal conductivity of heat pipe obtained from the heat transport equations was compared with the lumped thermal resistance network model. The maximum thermal conductivity obtained using the analytical model showed reasonable agreement with the experimental thermal conductivity. Maydink et al. [2] developed loop heat pipe for high heat transfer capacity using ammonia. Study was conducted for horizontal orientation. At a cooling temperature of 20 °C, a maximum heat load of 1700 W was achieved at a vapour temperature of 62 °C. Lin et al. [3] has studied thermal characteristics of long heat pipe using ammonia which is capable of dissipating 350 W at temperatures from 40 to 60 °C. Jasvanth et al. [4] developed loop heat pipe using ammonia with evaporator length 2.5 m and inside diameter 4.57 mm. A maximum heat dissipation capacity of about 600 W was achieved at a vapour temperature of 40.3 °C for 5 °C condenser temperature. Kcuck [5] studied the effects of three

---

V. Saravanan (✉)

Department of Mechanical Engineering, IIT Kharagpur, Kharagpur, India

K. Rakshith · Vishakh · N. Bhaskar · N. Badiger

Department of Mechanical Engineering, BNMIT, Bangalore, India

different working fluids, namely water, ammonia and mercury on performance of heat pipe. Two commonly used wick structures were also selected to demonstrate the wick structure effect on the heat transfer capacity of the heat pipe such as wire screen mesh and groove mesh. The study shows that it is preferable to use wire screen meshes with two layers of 24 meshes/inch. The performance of a heat pipe using a thermal resistance networking model was studied by Seo et al. [6], and the effect of the heat pipe length was also analysed. One-dimensional numerical simulations were conducted to verify the operating limits, and it was found that the capillary limit was the dominant limit that determined the heat transport capacity of the heat pipe. The effect of operating temperature and the fill ratios for heat pipes was presented by Mozumder and Chowdhury [7], The study reveals that the saturated boiling temperature, latent heat of vaporisation, evaporator surface temperature, working fluids and their fill ratios play a vital role in determining the heat transport capacity of the heat pipe. Faghri and Harley [8] studied the transient effects of heat pipes.

From the literature survey, it is observed that a majority of study is conducted on influence of wick properties, working fluid, heat pipe length and the filling ratios on the performance of the heat pipe. A thorough evaluation of the ideal temperature range of the capillary limit needs to be made, for it being the major factor in determining the thermal performance of a HPHS at lower temperatures. There also lies a scope to design a HPHS with a pre-determined thermal dissipation capacity to meet the global demand. In the present work, a heat pipe heat sink is designed and tested to dissipate a pre-determined thermal dissipation capacity.

## 2 Methodology

The experimental setup, schematically represented in Fig. 1 consists of the heat pipe heat sink (HPHS), heating element, thermocouples, data logger, power supply and

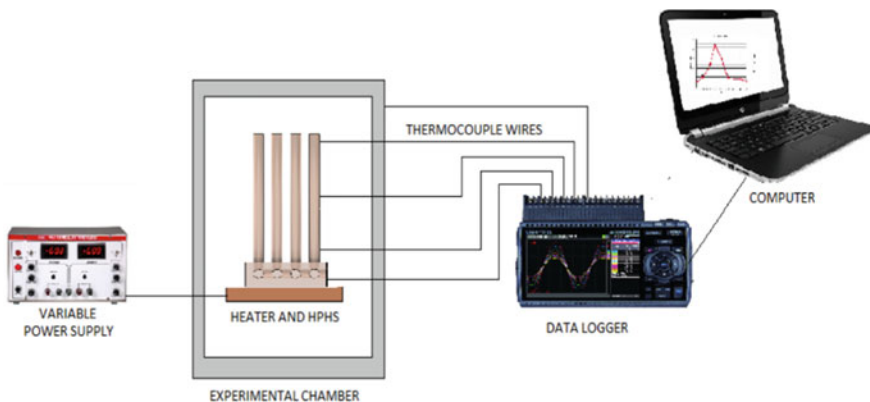


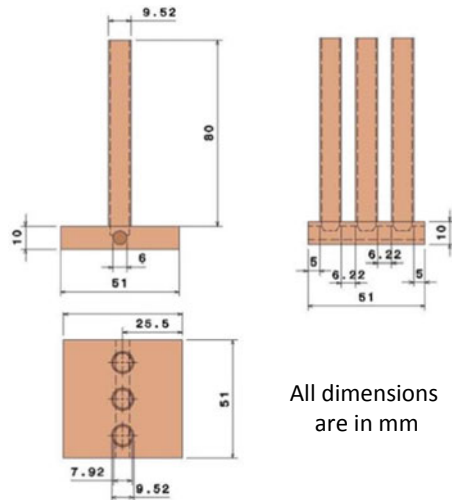
**Fig. 1** Schematic representation of experimental setup

the external experiment chamber. To record the temperature data, a set of three K-type thermocouples, placed along the length of random pipes are used in conjunction with a data logger. All thermocouples are equally spaced along the length of the HPHS and mounted using Kapton tape. The data logger is set to log data at a sampling rate of 1000 ms throughout the start-up, steady state and shut down of the HPHS as well as the conventional heat sink.

### 2.1 Experimental Details

The heat pipe heat sink assembly consists of common manifold made of copper which acts as base of the HPHS where heat pipes are attached to it. This common manifold is considered to be a common evaporator section of dimensions 51 mm × 51 mm × 10 mm. The manifold contains a channel of 6 mm diameter drilled through it to attach vacuum and charging port. The top face of the manifold consists of three holes along the centre of 9.52 mm diameter up to a depth of 8 mm. The heat pipes are placed inside these holes as shown in Fig. 2. Copper tubes of 10 mm outer diameter, 0.8 mm thickness and 80 mm length are used. The stainless-steel wick is inserted into the copper tubes after which they are capped at one end. Stainless-steel mesh is used which has as the wick material ( $9.9 \times 10^{-10} \text{ m}^2$  permeability and 44.08% porosity) with a wire diameter of 0.210 mm and a wire opening of 0.415 mm. The charging port is used to aid the vacuuming and evacuation of the PHS to a desired vacuum pressure.

**Fig. 2** Heat pipe heat sink test setup



All dimensions are in mm

### 2.2 Theoretical Modelling

Analytical computation was performed for two different working fluids, namely methanol and water at 60 °C to evaluate heat dissipation rate using following Eq. (1). The thermos physical properties of water and methanol are considered at 60 °C

$$\frac{2\sigma}{r_c} + \rho_l g L_t \geq \frac{16\mu_v L_{eff} Q}{2r_v^2 A_v \rho_v h_{fg}} + \frac{\mu_l L_{eff} Q}{K A_l \rho_l h_{fg}} + \rho_l g d_v \tag{1}$$

Wire mesh specification: Wire diameter  $d_w = 0.210$  mm, wire opening  $w = 0.415$  mm

Porosity,

$$\varepsilon = \frac{w^2}{(d_w + w)^2} \tag{2}$$

Permeability,

$$K = \frac{d_w^2 \varepsilon^3}{122(1 - \varepsilon)^2} \tag{3}$$

Capillary radius,

$$r_c = \frac{d_w + w}{2} \tag{4}$$

Effective length,

$$L_{eff} = \frac{L_e + L_c}{2} + L_a \tag{5}$$

$L_e, L_c$  and  $L_a$  are evaporator, condenser and effective length, respectively.

Number of turns of mesh  $N = 3$  turns

Mesh thickness,

$$t_w = 2d_w N \tag{6}$$

Area of the vapour section  $A_v = 2.2902 \times 10^{-5}$  m<sup>2</sup>.

Area of the liquid section  $A_l = 2.6362 \times 10^{-5}$  m<sup>2</sup>.

Total length of the pipe  $L_t = 80 \times 10^{-3}$  m.

Heat dissipated,  $Q$  methanol  $\leq 110$  W,  $Q$  water  $\leq 306.6$  W. Since water has a better heat transport capacity when compared to methanol at the given temperature, it is chosen as the working fluid for the HPHS.

### 3 Results and Discussion

In the present work, the thermal performance of HPHS is studied for five different heat inputs of 100, 150, 200, 250 and 300 W at a fill ratio of 60, 80 and 100%. The working fluid used for the experimental analysis is distilled water. The performance of the HPHS is studied based on temperature vs time graph, which is obtained from the experimental work. The difference in temperature across the axial length of the heat pipe is measured to verify the proper working condition at the steady state.

Figure 3 represents the temperature distribution across the length of the HPHS at 100 W for a fill ratio of 60%. The start-up, steady-state and shut down characteristics are depicted in the graph. Thermocouples are placed along the axial length of the heat pipe at lengths of 10 mm, 40 mm and 70 mm from the base. These are represented by bottom, middle and top positions in the graph. The following setup remains the same throughout all the test cases. The graph clearly shows that the HPHS is able to dissipate the heat that is generated by the nichrome resistance heater, which is in contact with the base of the HPHS. It is observed that there is very minimal temperature difference across the axial length of the heat pipe during the steady state which proves the fact that the HPHS is working under the capillary regime in the given conditions. Once the temperature goes beyond 90 °C, there is small variation in the temperature difference along the length of the heat pipe which may be attributed to other parameters like boiling limit coming into picture.

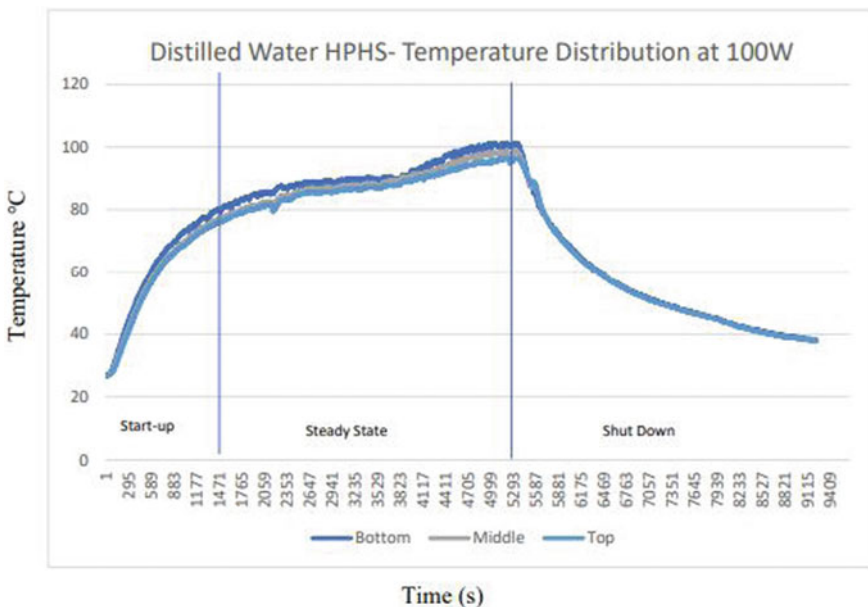


Fig. 3 Temperature distribution of HPHS at 100 W

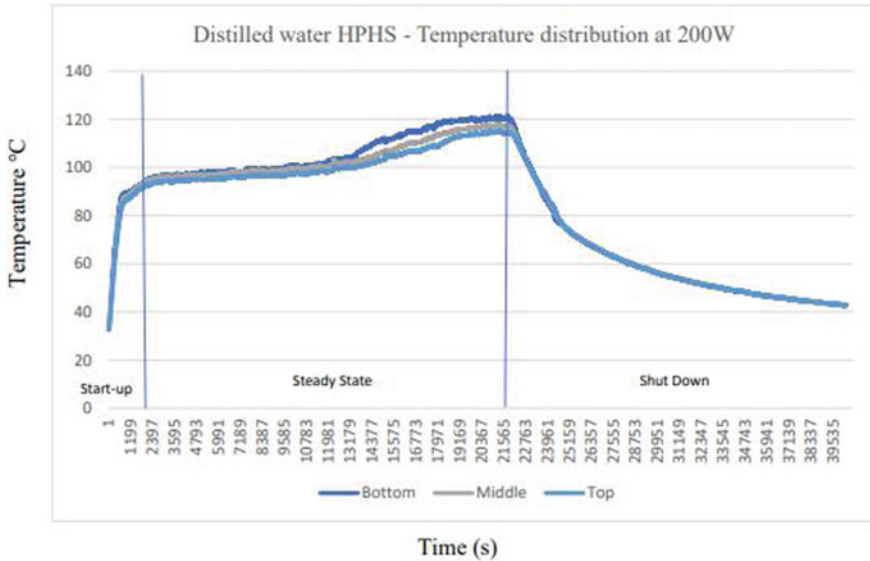


Fig. 4 Temperature distribution of HPHS at 200 W

Figure 4 represents the temperature distribution across the length of the HPHS at 200 W at a fill ratio of 100%. The start-up, steady-state and shut down characteristics are depicted in the graph. The graph obtained shows that the HPHS is able to dissipate the heat that is generated by the heater up to a certain point in the steady-state region. There is very minimal temperature difference across the length of the heat pipe until it reaches 100 °C in the steady-state region. After the temperature goes beyond 100 °C, there is significant variation in the temperature difference along the length of the heat pipe which may be caused due to the nucleate boiling of water that takes place due to the boiling limit and the shear force exerted by the vapour on the liquid at the wick surface that hinders the heat transport capacity.

Figure 5 represents the temperature distribution across the length of the HPHS at 250 W at a fill ratio of 100%. The graph obtained shows that there is significant temperature difference between the evaporator and the condenser section of the HPHS right at the beginning of the steady state. This trend continues throughout the steady state with the evaporator and the adiabatic section temperatures remaining close to each other, whereas the condenser section temperature lags by a small amount. After the temperature goes beyond 130 °C, the adiabatic section temperature goes beyond that of the evaporator section, hinting to the fact that the HPHS breakdown has occurred.

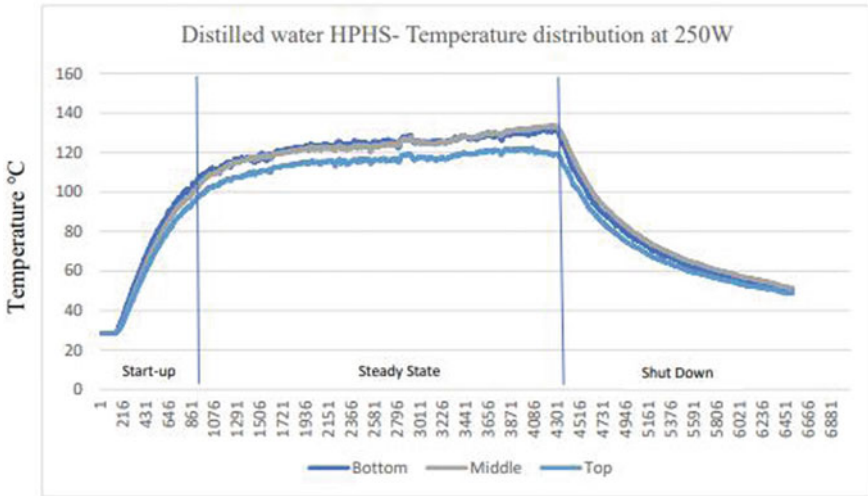


Fig. 5 Temperature distribution of HPHS at 250 W

### 4 Conclusions

A heat pipe heat sink has been designed and developed for electronic cooling application, and its thermal performance has been studied. The following conclusions can be drawn from the present study: (i) The present HPHS array is able to dissipate heat up to 250 W without undergoing any breakdown. (ii) There is a significant increase in the heat transport capacity of the HPHS on increasing the fill ratios up to a certain working temperature limit. (iii) The working fluid plays a significant role in determining the transport capacity in the working temperature considered with water being the best, as it has the highest latent heat among all other fluids that are suitable for operating conditions between 30 and 140 °C. (iv) Some of the major design parameters that needs to be considered while developing a HPHS are the wick structure, and the diameter of the vapour section of the heat pipe as both of them have a significant role is determining the heat transport capacity of the HPHS.

Figure 6 represents the temperature distribution across the length of the HPHS at 300 W at a fill ratio of 100%. The graph obtained shows that although there is very minimal temperature difference along the length of the heat pipe throughout the analysis, the adiabatic section temperature is higher than that of the evaporator section over the entire steady-state region. This shows that the HPHS is not working as theoretically predicted at 300 W, and it breaks down at high heat inputs beyond 250 W.

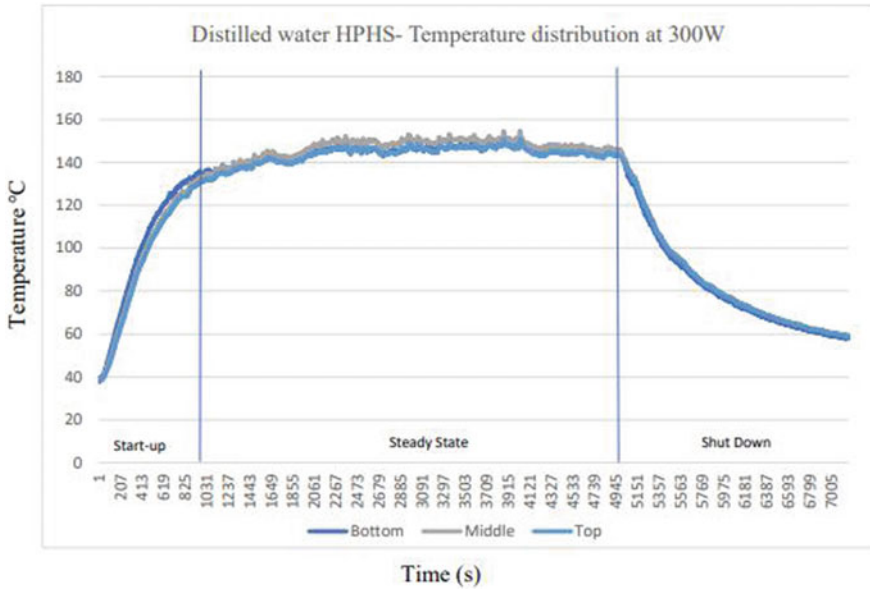


Fig. 6 Temperature distribution of HPHS at 300 W

**References**

1. Solomon AB, Sekar M, Yang SH (2016) Analytical expression for thermal conductivity of heat pipe. *Appl Therm Eng* 100:462–467
2. Maydanik Y, Pastukhov V, Chernysheva M (2018) Investigation of a loop heat pipe with a high heat transfer capacity. *Appl Therm Eng* 1052–1061
3. Lin G, Li N, Bai L, Wen D (2010) Experimental investigation of a dual compensation chamber loop heat pipe. *Int J Heat Mass Transf* 53:3231–3240
4. Jasvanth VS, Adoni A, Jaikumar V, Ambiraja A (2017) Design and testing of an ammonia loop heat pipe. *Appl Therm Eng* 111:1655–1663
5. Kcuck S (2007) A comparative investigation of heat transfer capacity limits of heat pipes. Graduate School of Natural and Applied Sciences
6. Seo YM, Park YG, Ha MY (2011) Effect of variation in length of the conventional heat pipe on the thermal performance. In: 13th International conference on heat transfer
7. Mozumder AK, Chowdhury MSH, Akon AF (2011) Characteristics of heat transfer for heat pipe and its correlation. *Int Sch Res Netw*
8. Faghri A, Harley C (1994) Transient lumped heat pipe analyses. *Heat Recovery Syst CHP* 14(4):351–363